A tridimensional model of the galactic interstellar extinction

Frédéric Arenou, M. Grenon, A. Gomez

Astron. Astrophys. 258, 104–111 (1992)

ASTRONOMY AND ASTROPHYSICS

16. A tridimensional model of the galactic interstellar extinction

F. Arenou[1], **M. Grenon**[2], **A. Gómez**[1]

[1] URA 335 du CNRS, Observatoire de Meudon, DASGAL, F-92195 Meudon, France
[2] Observatoire de Genève, CH-1290 Sauverny, Switzerland

Received July 18, 1991; accepted January 24, 1992

Abstract. The distribution of interstellar extinction has been mapped over the whole sky, using all available spectral and photometric data. The colour excess distribution is modelled as a function of galactic latitude, longitude and distance within about 1 kpc from the Sun. The model was used to predict the reddened Tycho and Johnson ($B - V$) colours, with the associated accuracy, from HD or MK spectral type and one magnitude (B or V), for stars without photoelectric photometry. This model is of special interest at intermediate and high galactic latitudes where colour excesses cannot be obtained from early type stars.

Key words: interstellar extinction – colour excess – intrinsic colours – photometry – Hipparcos

1. Introduction

In order to achieve the announced accuracy on the astrometric parameters expected from Hipparcos, photometric information was required to allocate the adequate observing time to each programme star. This time is a function of the magnitude called H_p – the star magnitude measured by the wide-band Hipparcos detector – which had to be estimated with an uncertainty smaller than 0.5 mag. The consequence of the large bandwith of the H_p magnitude is its dependence not only on the visual apparent brigthness of a star, but also on its colour ($B - V$) (Grenon 1989). In spite of the enormous effort made within the INCA Consortium to obtain new ground-based photoelectric measurements (Grenon 1989), about half of Hipparcos stars has no photoelectric photometry and the available B and V magnitudes come from inhomogeneous sources.

The main mission detector is potentially able to produce very high accurate photometry of programme stars provided that ageing effects on the optics are properly corrected through an on-orbit calibration. These effects are chromatic and the reduction to a standard system is possible only through the knowledge of accurate colours. Ideally the precision on ($B - V$) should be better than 0.04 mag in order to maintain a precision on H_p better than 0.003 mag through the mission.

The colours of stars without photoelectric photometry are far too inaccurate when deduced from blue photographs and photovisual magnitudes both for the H_p prediction and the photometric calibration. A serious improvement of the precision on colours may be expected by using the spectral classification, provided that the colour excess is sufficiently well mapped as a function of the galactic coordinates and distances.

The distribution of colour excess and interstellar reddening material in the solar neighborhood has been studied by several authors, notably by Lucke (1978), FitzGerald (1968) and Neckel & Klare (1980). These previous results were not useful for our purpose: they are presented in a graphical form and give no or poor information about the mean colour excesses outside the Galactic plane. Using all available spectral and photoelectric data contained in the INCA Database (Gómez et al. 1989; Turon et al. 1991), an analytical three dimensional model of the galactic interstellar extinction has been built and compared with results found in the literature.

For each spectral type, and luminosity class in case of MK classification, the colours deduced from the model were compared with photoelectric data. Systematic differences as functions of the colour excess were used to correct the intrinsic colours and to tune the model.

The method was applied to about 130 000 stars without photoelectric photometry, among which 60 000 stars are in the Input Catalogue. The validity of the procedure was finally checked by comparing calculated colours with the preliminary colours obtained from the star mappers of the Hipparcos satellite.

2. The data

The present study used all the stars contained in the INCA Database having at the same time spectral types (MK or HD) and B, V photometry. The choice of Johnson B, V photometry, instead of Geneva, Strömgren or Walraven photometry, is simply due to the large size of the final available sample.

The INCA Database contains the 215 000 stars proposed by the astronomical community to be observed by Hipparcos and a basic list of bright stars ('survey') required for satellite operation and data reduction. Some catalogues established for astrophysical purposes are highly represented, e.g. the Catalogue of extinction data (Neckel et al. 1980) and the Michigan Spectral Survey (Houk & Cowley 1975; Houk 1978, 1982).

During the preparation of the Hipparcos Input Catalogue, all the spectroscopic data available in SIMBAD (the Database of the Strasbourg Stellar Data Center) (Egret 1985) were incorporated into the INCA Database. Spectral types were mainly obtained from SIMBAD plus those published more recently in the Fourth volume of the Michigan Spectral Survey (Houk 1988). Other classifications published in the literature were also included. Finally, about 77 000 stars had a MK spectral type and 94 000 stars a HD spectral type.

Send offprint requests to: F. Arenou

Table 1. Number of stars with MK spectral type (26 052 stars)

Class \ Sp.	O	B	A	F	G	K	M
I	15	455	67	75	65	47	12
II	9	846	81	113	146	167	14
III	23	1554	505	463	1269	3061	341
IV-V	81	4340	2873	5661	2502	1063	125
VI	7	2	1	45	19	1	4

Table 2. Number of stars with HD spectral type (16 569 stars)

Spectral type	Number	Spectral type	Number
dO	28	dG	1211
dB	1774	gG	984
dA	4961	gK	2066
dF	5407	gM	138

Photoelectric photometry published in the seven major systems was extracted from the Database maintained at Lausanne Institute of Astronomy and completed with the newly observed measurements obtained in the framework of the INCA Consortium (Grenon 1989). Through adequate transformation equations, all data were expressed in terms of Johnson B, V, Tycho B_T, V_T and Hipparcos H_p magnitudes. A total of 58 000 colours were available for the model construction.

The final sample contains neither variable stars nor doubles closer than 10 arcsec. No special selection to limiting apparent magnitude was made, but the INCA Database does not contain stars fainter than V = 13 mag. Tables 1 and 2 give, respectively, the number of stars with MK and HD spectral types having photoelectric photometry.

Stars having MK spectral types were used to build the interstellar extinction model (see Sect.3) while the whole sample was used to estimate the colour index $(B-V)$ (see Sect.4). In the case of stars with HD classification, the following luminosity classes have been adopted: stars earlier than type G5 were considered as dwarfs (V), otherwise as giants (III).

3. The galactic interstellar extinction model

Previous work on this subject (op.cit.) clearly showed that the galactic interstellar extinction is a function of the position in the Galaxy (r: heliocentric distance and l_{II} and b_{II}: galactic coordinates). Analytical three dimensional models do not exist, probably due to the difficulty of modelling with small samples the reddening material distribution up to about 2 kpc. It is well known that the Parenago formula (Parenago 1940) as well as the cosecant law do not reproduce the observed interstellar monochromatic extinction. Using a large sample of stars having MK spectral types and photoelectric photometry in the spectral range O to F8 (about 17 000 stars), which constitutes a sub-sample of the data described in Sect. 2, the sky has been divided in cells and for each cell an analytic expression of the interstellar monochromatic extinction at V-magnitude $A_V(r, l_{II}, b_{II})$ has been obtained.

For each star the distance r and the visual extinction A_V have been computed using the well-known relations:

$$E_{B-V} = (B-V)_{ph} - (B-V)_0 \quad (1)$$

$$R = 3.30 + 0.28(B-V)_0 + 0.04E_{B-V} \quad (2)$$

$$A_V = R\,E_{B-V} \quad (3)$$

$$r = 10^{(V-M_V+5-A_V)/5} \quad (4)$$

where $(B-V)_{ph}$ is the photoelectric colour index, M_V and $(B-V)_0$ are the absolute magnitude and the intrinsic colour index respectively. The factor R depends upon the amount of reddening, the energy distribution in the stellar spectrum and the position in the Milky Way. The M_V and $(B-V)_0$ calibrations versus spectral type and luminosity class and the R formula quoted before were taken from Schmidt-Kaler (1982). From Eq. (1)-(3), the uncertainty of A_V is about 0.15 mag, depending primarily of the error on $(B-V)_0$. Assuming an uncertainty on M_V of roughly 0.5 mag, the relative error on the distance is 25%.

The sky has been divided in 199 cells in galactic coordinates and their boundaries were chosen following the Fig. 3 of Lucke (1978). Our goal was to derive an analytic expression for A_V, as a function of the distance and the galactic coordinates, representative of the general trend of the interstellar extinction and not of the local irregularities. The graphics shown by Neckel & Klare (1980) suggest that A_V could be represented in a first approximation by a quadratic relationship. In each cell, the following quadratic relation has been adopted up to a distance r_0:

$$A_V(r, l_{II}, b_{II}) = \alpha(l_{II}, b_{II})r + \beta(l_{II}, b_{II})r^2, \qquad \text{if } r \le r_0 \quad (5)$$

where r_0 represents the distance limit of the absorbing layers[1] . As a first estimate $r_0 = r_{thick} = 0.2/\sin|b_{II}|$ was taken, 0.2 kpc being the adopted half thickness of the galactic plane. As it is shown later, the definition of r_0 depends on the studied region. For the regions $|b_{II}| < 5°$, r_{thick} was fixed equal to 2 kpc. Out of the absorbed regions A_V should remain constant and identically to $A_V(r_0, l_{II}, b_{II})$. In the case of cells including a large part of the galactic plane, $|b_{II}| < 15°$ regions, a better representation of the interstellar extinction was obtained adopting beyond r_0 the following linear regression relation:

$$A_V(r, l_{II}, b_{II}) = A_V(r_0, l_{II}, b_{II}) + \gamma(l_{II}, b_{II})(r - r_0) \quad (5bis)$$

In order to adopt in each cell the best r_0 value, some constraints on A_V have been taken into account. For instance, A_V cannot diminish with r. Figs. 1a and 1b show that A_V arrives at a maximum value for $r = r_{dec}$ and then decreases. This decreasing is spurious, and is related to the presence of higher interstellar extinction and to the lack of fainter stars in the sample. On the other hand, A_V has not to go beyond the largest observed value in a given direction, corresponding to a distance $r = r_{larg}$ in Figs. 1a and 1b. Moreover, this last maximum observed value has to be compared with the results found in the literature. We adopted:

$A_{max} = 0.1$, if $60° \le |b_{II}| < 90°$
$A_{max} = 1.2$, if $45° \le |b_{II}| < 60°$
$A_{max} = 3.0$, if $|b_{II}| < 45°$

The corresponding distance called r_{max} is absent from Figs. 1a & 1b because it is reached at r = 9 kpc in the example shown in Fig. 1a and never reached in the other case.

Consequently, the r_0 value used in formulae (5) and (5bis) corresponds to the smallest A_V value between $A_V(r_{thick})$, $A_V(r_{dec})$, $A_V(r_{larg})$ and $A_V(r_{max})$, r_0 being $\le r_{dec}$. The regression coefficients α, β and γ have been determined using the least square method

[1] If the parabola decreases at the beginning (from $r = 0$) and then increases, A_V takes negative values in a distance interval. In these few cases, we adopted $A_V \equiv 0$ in this interval.

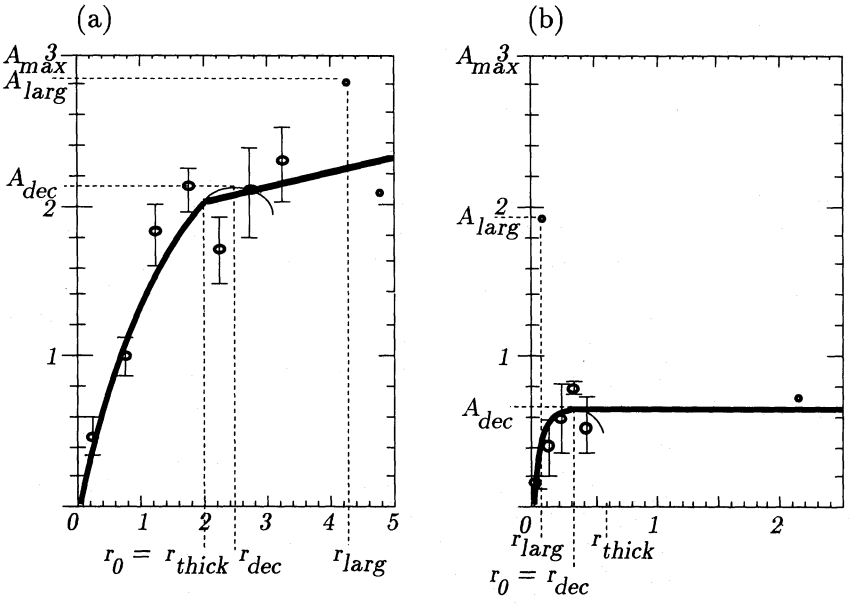

Fig. 1. Absorption (mag) as a function of distance (kpc): Example in the galactic plane ($180° \leq l_{II} < 190°$, $-5° \leq b_{II} < 5°$, bins of 500pc) (a) and at intermediate galactic latitude ($20° \leq l_{II} < 40°$, $15° \leq b_{II} < 30°$, bins of 100pc) (b)

and are given for each cell in Appendix; the r_0 values are also indicated. The last column gives the relative error $\frac{\sigma_{A_V}}{A_V}$, expressed in percentages. For each star, the error on the computed $A_V(r)$ has been estimated by $\sqrt{0.15^2 + (\frac{\sigma_{A_V}}{A_V} A_V(r))^2}$, where 0.15 mag is the assumed uncertainty of A_V calculated from Eq. (1)-(3). High relative errors ($> 100\%$) may exist in cells containing a few number of stars or where the obtained extinction is small compared to the size of the computed error. This last case could be the result of irregularities of the distribution of the interstellar matter. The average relative error on the whole sky is about 35%.

One may ask how well our model compares with previous studies in small regions. Due to the relatively large sizes of the cells, this comparison has little meaning. The model gives the general trend of the interstellar extinction in each region and does not take into account the irregularities of the distribution of the absorbing material. On the other hand, we expect in general, for small distances ($r \leq$ 200pc), a slightly overestimation of A_V. This fact is shown in Fig. 2 which gives the comparison between the visual extinction in the Johnson UBV-System calculated using Walraven photometry for the region of Upper-Centaurus Lupus subgroup (de Geus et al. 1989) and our model's values. However, the overestimation of A_V can be considered negligible if we take into account the estimated errors on A_V. We have also compared our results with those of Neckel and Klare (1980) : for regions having $A_V < 0.5$ mag the agreement is very satisfactory, otherwise it depends on the irregularities of the distribution of the interstellar matter in the cell.

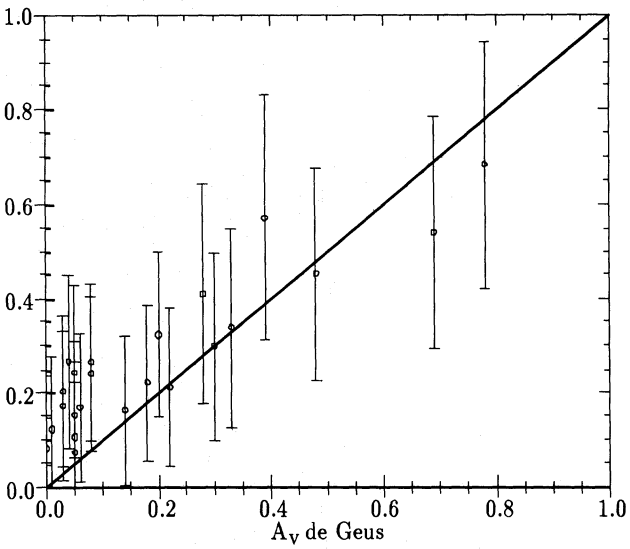

Fig. 2. Estimated $A_V(r)$ versus A_V from de Geus et al. (1989) in the Upper-Centaurus Lupus region.

4. $(B - V)$ colour index estimation

For each of the stars given in Tables 1 and 2 the (B-V) colour index has been estimated using the interstellar extinction model described in section 3. This colour index, called $(B - V)_{red}$, has been compared to $(B - V)_{ph}$. The distribution of the differences $\delta_{B-V} = (B - V)_{red} - (B - V)_{ph}$ has been evaluated as a function of the spectral type and the luminosity class. The $\overline{\delta}_{B-V}$ values in four bins of E_{B-V} are given in Tables 3 and 4, corresponding to stars having MK and HD classification respectively. The stars having $E_{B-V} > 0.35$ or $|\delta_{B-V}| > 0.75$ mag were not included. We expect to obtain $\overline{\delta}_{B-V}$ values approximatively null. In general, they increase with the colour excess and for late spectral types. These figures are the systematic corrections to be applied to the $(B - V)_{red}$ colour index in order to estimate the corresponding $(B - V)$ colour index. The rms error σ_{B-V}, given in the Tables, is the error on the colour index. It includes the errors in the distance determinations, in the adopted intrinsic colour indexes and in the spectroscopic and photometric data. These errors obtained on the estimated colour indexes are mostly smaller than 0.15 mag for MK stars and 0.2 mag for HD stars. These results allowed us to apply the method to stars without photoelectric photometry.

To summarize the colour estimation process, given a star with a V magnitude (or a B magnitude, as $V = B-(B-V)_0-E_{B-V}$) and M_V, $(B-V)_0$ derived from its spectral type, Eqs. (2)-(4) are iterated, beginning with $A_V = 0$ and then with $A_V(r)$ given in appendix. This

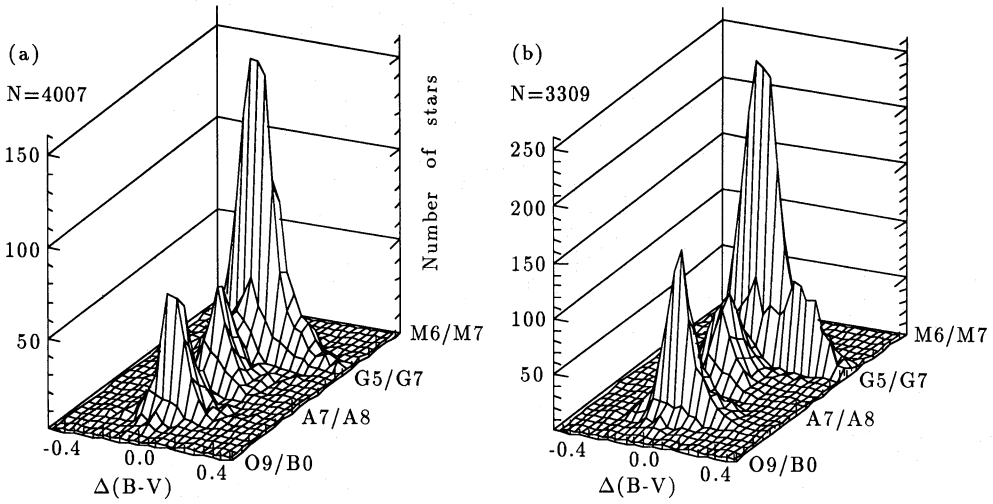

Fig. 3. Distribution of differences between $(B-V)_{NDAC}$ and $(B-V)_{INCA}$ and spectral types, for stars with MK spectral type (a) and for stars with HD spectral type (b)

Table 3. Corrections on $(B-V)$ and precision on $(B-V)$ as a function of spectral type, luminosity class and bins of colour excess, for stars with MK spectral type

	$E_{B-V} \leq .05$		].05, .15]		].15, .25]		].25, .35]	
	$\overline{\delta}_{B-V}$	σ	$\overline{\delta}_{B-V}$	σ	$\overline{\delta}_{B-V}$	σ	$\overline{\delta}_{B-V}$	σ
B I	.030	.15	.025	.110	.020	.164	.030	.170
A I	.050	.15	.030	.054	.000	.165	.000	.111
F I	-.060	.133	-.060	.162	-.060	.080	-.060	.115
G I	.040	.203	.030	.081	.040	.085	.090	.164
K I	.080	.081	.030	.168	.030	.137	.090	.237
M I	-.020	.15	-.020	.15	-.020	.15	-.020	.106
B II	.010	.057	.040	.093	.060	.104	.040	.156
A II	-.070	.102	-.070	.142	-.050	.138	-.020	.165
F II	-.010	.060	-.020	.118	-.010	.111	.050	.169
G II	.030	.145	.020	.141	.060	.122	.160	.114
K II	.020	.117	.030	.147	.090	.170	.200	.25
M II	.080	.10	.070	.088	.120	.20	.240	.25
B III	.005	.054	.015	.081	.015	.104	.015	.124
A III	-.015	.069	-.020	.099	-.020	.15	-.020	.152
F III	.010	.067	.010	.107	.020	.15	.030	.25
G III	.020	.15	.030	.142	.030	.156	.030	.377
K III	-.020	.12	-.010	.134	.000	.214	.000	.232
M III	.025	.063	.025	.092	.025	.115	.025	.198
BIV,V	.005	.055	.010	.064	.005	.095	.000	.128
AIV,V	-.010	.061	.000	.10	-.010	.106	-.020	.122
FIV,V	-.005	.10	-.005	.071	.000	.15	.000	.25
GIV,V	.000	.096	.020	.133	.040	.118	.060	.20
KIV,V	-.040	.150	-.040	.239	-.040	.25	-.040	.25
MIV,V	.040	.133	.040	.20	.040	.25	.040	.25
F VI	.010	.053	.010	.035	.000		.000	
G VI	.070	.110	.000		.000		.000	

gives E_{B-V}, and finally the colour index $(B-V) = (B-V)_0 + E_{B-V} - \overline{\delta}_{B-V}$ and its associated error.

Table 4. Corrections on $(B-V)$ and precision on $(B-V)$ as a function of spectral type and bins of colour excess, for stars with HD spectral type

	$E_{B-V} \leq .05$		].05, .15]		].15, .25]		].25, .35]	
	$\overline{\delta}_{B-V}$	σ	$\overline{\delta}_{B-V}$	σ	$\overline{\delta}_{B-V}$	σ	$\overline{\delta}_{B-V}$	σ
dB	-.025	.093	.005	.1	-.005	.139	-.035	.180
dA	-.080	.15	-.020	.14	.020	.141	.000	.155
dF	-.025	.072	.005	.107	.010	.1	.000	.15
dG	-.030	.126	.000	.155	.090	.086	.220	.20
gG	.070	.195	.090	.198	.220	.209	.330	.178
gK	-.040	.197	.020	.218	.080	.243	.260	.317
gM	.010	.082	.010	.143	.010	.20	.010	.170

5. Comparison with the preliminary data obtained with the Hipparcos star mappers

Even if the model described above is self-consistent, it is worth comparing the colours predicted within the INCA consortium, $(B-V)_{INCA}$, with those obtained from the preliminary measurements coming from the NDAC reduction consortium (van Leeuwen et al. 1992). These data are the result of the analysis of 12 weeks of observation from the Hipparcos star mappers; as they are B_T and V_T magnitudes in the Tycho bands (Grenon et al. 1992), they must beforehand be transformed to Johnson magnitudes. Moreover, for a safe comparison, we kept only the stars with $|V_{NDAC} - V_{INCA}| < .05$ in order to reduce the errors in the estimation of the distance, and thus in the reddening. Figure 3 shows the distribution of $\Delta(B-V) = (B-V)_{NDAC} - (B-V)_{INCA}$ separately for the stars with MK spectral type and HD spectral type. This figure provides the distributions of the spectral types of the stars in the samples as well as the distribution of $\Delta(B-V)$ for each spectral type; each bin is 0.04 in mag and about 2 in spectral subtypes (from O9/B0 to M6/M7). As we can see, the distributions of $\Delta(B-V)$ are centered near 0., with mean/standard deviation of $-.008/0.091$ for stars with MK spectral type and $0.02/0.17$ for stars with HD spectral type. The distribution is clearly asymmetric for HD spectral type G5. This type contains a mixture of giants and dwarfs with $(B-V)_0 = 0.88$ and 0.68 respectively. The ratio dwarfs/giants is a function of distance and b_{II}; the distribution tail is due to giants. For the other stars, and this is

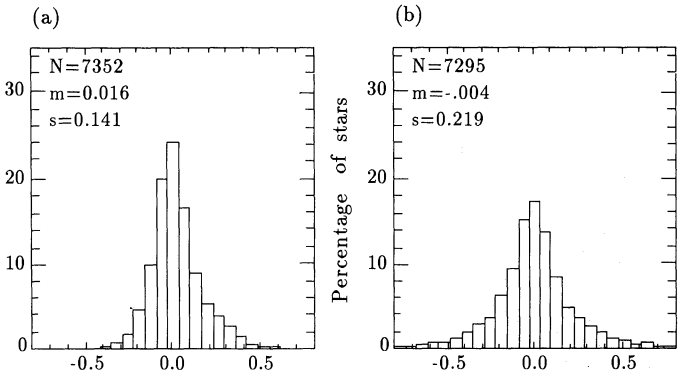

Fig. 4. Distribution of differences between $(B-V)_{NDAC}$ colour index and computed colours (a) and of differences between $(B-V)_{NDAC}$ and colours deduced from B and V magnitudes coming from heterogeneous sources (b)

also true for stars with MK spectral type, we may still notice a small tail towards $\Delta(B-V) > 0$. This is because the concerned stars are fainter, farther than about 1kpc and the estimated interstellar extinction is probably underestimated. However, all these effects had been accounted for in the $(B-V)$ error bars.

We may now ask: what would be the differences $\Delta(B-V)$ if we had not built the extinction model, that is in using $B-V$ colours with B & V magnitudes coming from heterogeneous sources. The answer is given in Fig. 4, where MK and HD stars are considered together. The number of stars is given as well as the mean and standard deviation of the differences. The slight asymmetry mentioned before is visible in Fig. 4a; however the improvement of colours with the extinction model is perfectly clear.

6. Comparison with extinction from H I distribution

At intermediate galactic latitudes, the total extinction, computed for each cell at $r = r_0$, may be compared to that deduced from surveys of neutral hydrogen (HI) column densities and deep galaxy counts. Maps of E_{B-V} contours by Burstein and Heiles (1982) were used to check both the asymptotic behaviour of the relations given in annex and the amplitude of the scatter due to irregularities of the interstellar matter distribution. In the galactic latitude ranges +15° to +45° and −45° to −15°, reddenings are read on a mesh of 9 to 12 points, depending on the cell size. Since the mapping precision and the reading resolution are about 0.01 to 0.02 mag, in moderately reddened areas the scatter in E_{B-V} is representative of the true irregularity of the interstellar matter distribution. Due to the rather large cell size, the irregularities lead to a ratio $\frac{\sigma_{A_V}}{A_V}$ of about 0.42, a value similar to that computed in well documented areas.

The comparison between the computed total mean colour excess E_{B-V} and those from Burstein and Heiles is given in Fig. 5 for the precited ranges of galactic latitudes. Considering the noise on both colour-excess determinations the agreement is quite satisfactory. Apart from a possible zero–point shift, there is some evidence for the observed E_{B-V} to be systematically larger by about 20% than those computed from HI.

In the north galactic cap, E_{B-V} is directly deduced from HI maps through the relation : $E_{B-V} = 0.485 N_H$ where N_H is given in units of 10^{15} atoms.cm^{-2}. The comparison of excesses for cells with b_{II} from +60° to +90° is given in Fig. 6. The differences between the two approaches are within 0.01 mag on E_{B-V}.

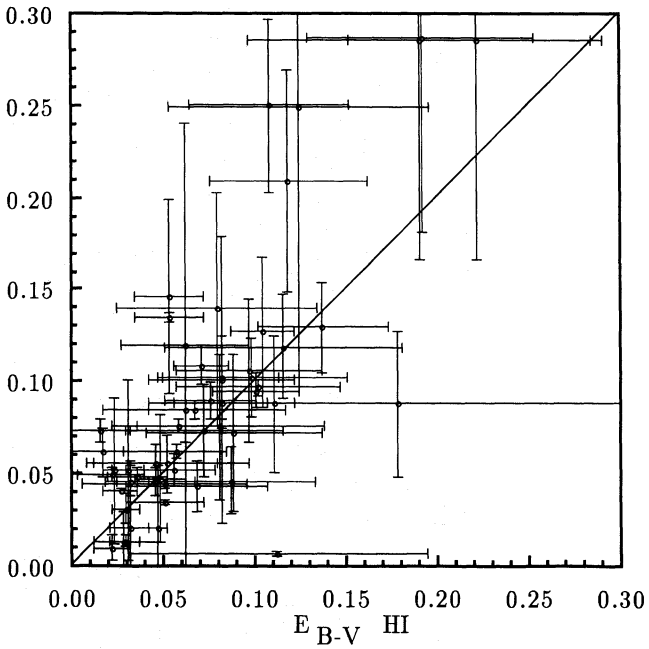

Fig. 5. Comparison between the total colour excesses $E_{B-V_{mod}}$ computed from the extinction model at $r = r_0$, and those read on maps of E_{B-V} built from HI distribution and deep galaxy counts from Burstein and Heiles. The ranges in galactic latitude are −45° to −15° and +15° to +45°.

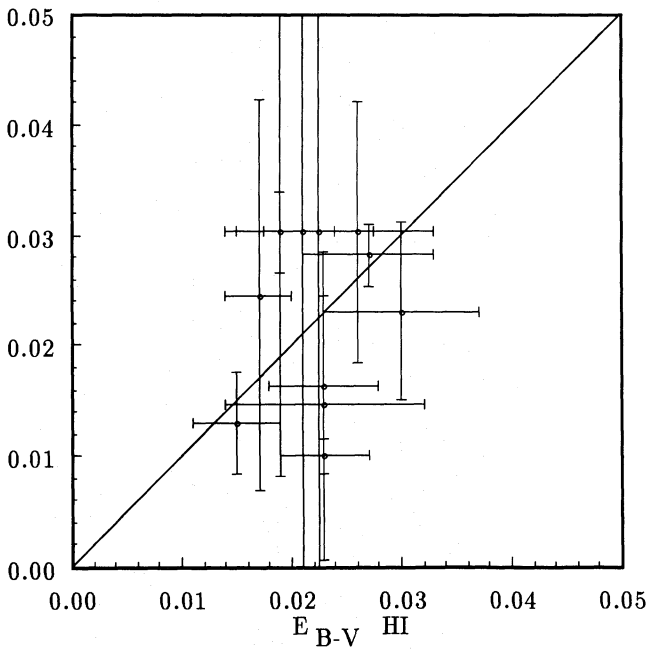

Fig. 6. Comparison between the total colour excesses E_{B-V} from the model and those from HI distribution in the north galactic cap ($b_{II} > 60°$).

7. Conclusion

The primary goal of the model was the production of colours (and ultimately instrumental magnitudes) for stars without photoelectric photometry to be observed by the Hipparcos satellite. Indeed it is of a more general application since it provides a three dimensional distribution of the reddening with a mean accuracy of about 40% for

stars within and outside the dust lane. It complements the existing description of the interstellar matter distribution for the intermediate and high galactic latitudes. This model gives the general trend of the interstellar extinction and does not take into account the local irregularities of the absorbing material; it should be used preferably for investigations of statistical character.

The C or FORTRAN source program may be obtained upon request at MESIOA::ARENOU (SPAN–DECNET) or ARENOU at FRMEU51 (EARN-BITNET).

Acknowledgements. We would like to thank the referee Dr Knude for his useful comments.

References

Burstein D., Heiles C., 1982, Astron. J., 1165
de Geus E.J., de Zeeuw P.T., Lub J., 1989, A&A 216,44
Egret D., 1985, ESA–SP 234, 105
FitzGerald M.P., 1968, AJ 73, 983
Gómez A., Morin D., Arenou F., 1989, ESA–SP 1111, 23
Grenon M., 1989, ESA–SP 1111, 129
Grenon M., Mermilliod M., Mermilliod J.C., 1992, A&A, this issue (paper 13)
Houk N., Cowley A.P., 1975, Michigan Catalog of Two Dimensional Spectral Types for the HD Stars, Vol 1, Ann Arbor
Houk N., 1978, Michigan Catalog of Two Dimensional Spectral Types for the HD Stars, Vol 2, Ann Arbor
Houk N., 1982, Michigan Catalog of Two Dimensional Spectral Types for the HD Stars, Vol 3, Ann Arbor
Houk N., 1988, Michigan Catalog of Two Dimensional Spectral Types for the HD Stars, Vol 4, Ann Arbor
van Leeuwen F. et al., 1992, A&A, this issue (paper 19)
Lucke P.B., 1978, A&A 64, 367
Neckel Th., Klare G., 1980, A&AS 42, 251
Parenago P., 1940, AZh 17,3
Schmidt-Kaler Th., 1982, in Landolt-Börnstein, Springer Verlag, vol. 2, p. 1
Turon C. et al., 1991, Databases & On-line Data in Astronomy, eds. M.A. Albrecht and D. Egret, p. 67

Appendix

Regression parameters for $A_V(r)$ and relative error on $A_V(r)$ by galactic longitude and latitude bins; α and γ in mag.kpc^{-1}, β in mag.kpc^{-2}, r_0 in kpc, $\frac{\sigma_{A_V}}{A_V}$ in %

-90≤ b_{II} <-60	α	β	r_0	γ	$\frac{\sigma_A}{A}$
0 ≤ l_{II} <29	2.22534	-6.00212	0.052	0.0	13
29 ≤ l_{II} <57	3.35436	-14.74567	0.035	0.0	40
57 ≤ l_{II} <85	2.77637	-9.62706	0.042	0.0	15
85 ≤ l_{II} <110	4.44190	-19.92097	0.025	0.0	36
110≤ l_{II} <150	4.46685	-26.07305	0.026	0.0	28
150≤ l_{II} <180	7.63699	-46.10856	0.014	0.0	38
180≤ l_{II} <210	2.43412	-8.69913	0.050	0.0	36
210≤ l_{II} <240	3.34481	-13.93228	0.035	0.0	38
240≤ l_{II} <270	1.40733	-3.43418	0.091	0.0	30
270≤ l_{II} <300	1.64466	-3.97380	0.074	0.0	28
300≤ l_{II} <330	2.12696	-6.05682	0.056	0.0	14
330≤ l_{II} <360	2.34636	-8.17784	0.052	0.0	16

-60≤ b_{II} <-45	α	β	r_0	γ	$\frac{\sigma_A}{A}$
0 ≤ l_{II} <30	2.77060	-9.52310	0.145	0.0	16
30 ≤ l_{II} <60	1.96533	-5.63251	0.174	0.0	06
60 ≤ l_{II} <110	1.93622	-13.31757	0.073	0.0	26
110≤ l_{II} <180	1.05414	-2.36540	0.223	0.0	74
180≤ l_{II} <210	1.39990	-1.35325	0.252	0.0	10
210≤ l_{II} <240	2.73481	-11.70266	0.117	0.0	08
240≤ l_{II} <270	2.99784	-11.64272	0.129	0.0	03
270≤ l_{II} <300	3.23802	-11.63810	0.139	0.0	07
300≤ l_{II} <330	1.72679	-6.05085	0.143	0.0	07
330≤ l_{II} <360	1.88890	-5.51861	0.171	0.0	14

-45≤ b_{II} <-30	α	β	r_0	γ	$\frac{\sigma_A}{A}$
0 ≤ l_{II} <30	1.98973	-4.86206	0.205	0.0	06
30 ≤ l_{II} <60	1.49901	-3.75837	0.199	0.0	16
60 ≤ l_{II} <90	0.90091	-1.30459	0.329	0.0	73
90 ≤ l_{II} <120	1.94200	-6.26833	0.155	0.0	18
120≤ l_{II} <160	-0.37804	10.77372	0.210	0.0	100
160≤ l_{II} <200	-0.15710	5.03190	0.294	0.0	24
200≤ l_{II} <235	3.20162	-10.59297	0.151	0.0	09
235≤ l_{II} <265	1.95079	-4.73280	0.206	0.0	21
265≤ l_{II} <300	1.91200	-4.97640	0.192	0.0	17
300≤ l_{II} <330	2.50487	-8.63106	0.145	0.0	28
330≤ l_{II} <360	2.44394	-9.17612	0.133	0.0	07

-30≤ b_{II} <-15	α	β	r_0	γ	$\frac{\sigma_A}{A}$
0 ≤ l_{II} <20	2.82440	-4.78217	0.295	0.0	32
20 ≤ l_{II} <40	3.84362	-8.04690	0.239	0.0	46
40 ≤ l_{II} <80	0.60365	0.07893	0.523	0.0	22
80 ≤ l_{II} <100	0.58307	-0.21053	0.523	0.0	53
100≤ l_{II} <120	2.03861	-4.40843	0.231	0.0	60
120≤ l_{II} <140	1.14271	-1.35635	0.421	0.0	34
140≤ l_{II} <160	0.79908	1.48074	0.523	0.0	61
160≤ l_{II} <180	0.94260	8.16346	0.441	0.0	42
180≤ l_{II} <200	1.66398	0.26775	0.523	0.0	42
200≤ l_{II} <220	1.08760	-1.02443	0.523	0.0	45
220≤ l_{II} <240	1.20087	-2.45407	0.245	0.0	06
240≤ l_{II} <260	1.13147	-1.87916	0.301	0.0	16
260≤ l_{II} <280	1.97804	-2.92838	0.338	0.0	21
280≤ l_{II} <300	1.40086	-1.12403	0.523	0.0	19
300≤ l_{II} <320	2.06355	-3.68278	0.280	0.0	42
320≤ l_{II} <340	1.59260	-2.18754	0.364	0.0	15
340≤ l_{II} <360	1.45589	-1.90598	0.382	0.0	21

$-15 \leq b_{II} < -5$	α	β	r_0	γ	$\frac{\sigma_A}{A}$
$0 \leq l_{II} < 10$	2.56438	-2.31586	0.554	0.0	37
$10 \leq l_{II} < 20$	3.24095	-2.78217	0.582	0.0	38
$20 \leq l_{II} < 30$	2.95627	-2.57422	0.574	0.08336	41
$30 \leq l_{II} < 40$	1.85158	-0.67716	1.152	0.0	04
$40 \leq l_{II} < 50$	1.60770	0.35279	0.661	0.0	24
$50 \leq l_{II} < 60$	0.69920	-0.09146	0.952	0.12839	02
$60 \leq l_{II} < 80$	1.36189	-1.05290	0.647	0.16258	45
$80 \leq l_{II} < 90$	0.33179	0.37629	1.152	0.0	62
$90 \leq l_{II} < 100$	1.70303	-0.75246	1.132	0.0	31
$100 \leq l_{II} < 110$	1.97414	-1.59784	0.618	0.12847	35
$110 \leq l_{II} < 120$	1.07407	-0.40066	1.152	0.17698	14
$120 \leq l_{II} < 130$	1.69495	-1.00071	0.847	0.08567	28
$130 \leq l_{II} < 140$	1.51449	-0.08441	0.897	0.0	12
$140 \leq l_{II} < 150$	1.87894	-0.73314	1.152	0.0	23
$150 \leq l_{II} < 160$	1.43670	0.67706	0.778	0.42624	03
$160 \leq l_{II} < 180$	6.84802	-5.06864	0.676	0.0	50
$180 \leq l_{II} < 190$	4.16321	-5.80016	0.359	0.60387	51
$190 \leq l_{II} < 200$	0.78135	-0.27826	1.152	0.0	04
$200 \leq l_{II} < 210$	0.85535	0.20848	1.152	0.0	17
$210 \leq l_{II} < 220$	0.52521	0.65726	1.152	0.0	07
$220 \leq l_{II} < 230$	0.88376	-0.44519	0.993	0.06013	40
$230 \leq l_{II} < 240$	0.42228	-0.26304	0.803	0.0	26
$240 \leq l_{II} < 250$	0.71318	-0.67229	0.530	0.20994	55
$250 \leq l_{II} < 260$	0.99606	-0.70103	0.710	0.01323	48
$260 \leq l_{II} < 270$	0.91519	-0.39690	1.152	0.01961	48
$270 \leq l_{II} < 280$	0.85791	-0.29115	1.152	0.0	19
$280 \leq l_{II} < 290$	1.44226	-1.09775	0.657	0.0	39
$290 \leq l_{II} < 300$	2.55486	-1.68293	0.759	0.0	31
$300 \leq l_{II} < 310$	3.18047	-2.69796	0.589	0.0	40
$310 \leq l_{II} < 320$	2.11235	-1.77506	0.595	0.0	29
$320 \leq l_{II} < 330$	1.75884	-1.38574	0.635	0.0	25
$330 \leq l_{II} < 340$	1.97257	-1.55545	0.634	0.00043	34
$340 \leq l_{II} < 350$	1.41497	-1.05722	0.669	0.03264	46
$350 \leq l_{II} < 360$	1.17795	-0.95012	0.620	0.03339	46

$-5 \leq b_{II} < 5$	α	β	r_0	γ	$\frac{\sigma_A}{A}$
$0 \leq l_{II} < 10$	2.62556	-1.11097	1.182	0.00340	57
$10 \leq l_{II} < 20$	3.14461	-1.01140	1.555	0.0	42
$20 \leq l_{II} < 30$	4.26624	-1.61242	1.323	0.0	34
$30 \leq l_{II} < 40$	2.54447	-0.12771	1.300	0.0	30
$40 \leq l_{II} < 50$	2.27030	-0.68720	1.652	0.04928	52
$50 \leq l_{II} < 60$	1.34359	-0.05416	2.000	0.0	32
$60 \leq l_{II} < 70$	1.76327	-0.26407	2.000	0.0	37
$70 \leq l_{II} < 80$	2.20666	-0.41651	2.000	0.0	36
$80 \leq l_{II} < 90$	1.50130	-0.09855	1.475	0.0	45
$90 \leq l_{II} < 100$	2.43965	-0.82128	1.485	0.01959	36
$100 \leq l_{II} < 110$	3.35775	-1.16400	0.841	0.00298	35
$110 \leq l_{II} < 120$	2.60621	-0.68687	1.897	0.0	36
$120 \leq l_{II} < 130$	2.90112	-0.97988	1.480	0.0	32
$130 \leq l_{II} < 140$	2.55377	-0.71214	1.793	0.0	38
$140 \leq l_{II} < 150$	3.12598	-1.21437	1.287	0.15298	23
$150 \leq l_{II} < 160$	3.66930	-2.29731	0.799	0.33473	40
$160 \leq l_{II} < 170$	2.15465	-0.70690	1.524	0.14017	37
$170 \leq l_{II} < 180$	1.82465	-0.60223	1.515	0.20730	29
$180 \leq l_{II} < 190$	1.76269	-0.35945	2.000	0.08052	28
$190 \leq l_{II} < 200$	1.06085	-0.14211	2.000	0.0	48
$200 \leq l_{II} < 210$	1.21333	-0.23225	2.000	0.0	57
$210 \leq l_{II} < 220$	0.58326	-0.06097	2.000	0.36962	30
$220 \leq l_{II} < 230$	0.74200	-0.19293	1.923	0.07459	48
$230 \leq l_{II} < 240$	0.67520	-0.21041	1.604	0.16602	49
$240 \leq l_{II} < 250$	0.62609	-0.25312	1.237	0.14437	73
$250 \leq l_{II} < 260$	0.61415	-0.13788	2.000	0.26859	42
$260 \leq l_{II} < 270$	0.58108	0.01195	2.000	0.07661	40
$270 \leq l_{II} < 280$	0.68352	-0.10743	2.000	0.00849	50
$280 \leq l_{II} < 290$	0.61747	0.02675	2.000	0.0	49
$290 \leq l_{II} < 300$	1.06827	-0.26290	2.000	0.0	44
$300 \leq l_{II} < 310$	1.53631	-0.36833	2.000	0.02960	37
$310 \leq l_{II} < 320$	1.94300	-0.71445	1.360	0.15643	36
$320 \leq l_{II} < 330$	1.22185	-0.40185	1.520	0.07354	48
$330 \leq l_{II} < 340$	1.79429	-0.48657	1.844	0.0	43
$340 \leq l_{II} < 350$	2.29545	-0.84096	1.365	0.0	32
$350 \leq l_{II} < 360$	2.07408	-0.64745	1.602	0.12750	36

$5 \leq b_{II} < 15$	α	β	r_0	γ	$\frac{\sigma_A}{A}$
$0 \leq l_{II} < 10$	2.94213	-2.09258	0.703	0.05490	41
$10 \leq l_{II} < 30$	3.04627	7.71159	0.355	0.0	45
$30 \leq l_{II} < 40$	3.78033	-3.91956	0.482	0.0	42
$40 \leq l_{II} < 50$	2.18119	-2.4050	0.453	0.0	27
$50 \leq l_{II} < 60$	1.45372	-0.49522	1.152	0.0	31
$60 \leq l_{II} < 70$	1.05051	-1.01704	0.516	0.0	02
$70 \leq l_{II} < 80$	0.48416	-0.27182	0.891	0.08639	94
$80 \leq l_{II} < 90$	0.61963	0.41697	1.152	0.47171	35
$90 \leq l_{II} < 100$	4.40348	-2.95611	0.745	0.0	52
$100 \leq l_{II} < 120$	2.50938	-0.56541	1.152	0.0	27
$120 \leq l_{II} < 130$	0.44180	1.58923	0.949	0.0	04
$130 \leq l_{II} < 140$	3.96084	-3.37374	0.587	0.34109	40
$140 \leq l_{II} < 160$	2.53335	-0.40541	1.152	0.0	38
$160 \leq l_{II} < 170$	2.03760	-0.66317	1.152	0.0	23
$170 \leq l_{II} < 200$	1.06946	-0.87395	0.612	0.29230	29
$200 \leq l_{II} < 210$	0.86348	-0.65870	0.655	0.09089	79
$210 \leq l_{II} < 230$	0.30117	-0.16136	0.933	0.07495	17
$230 \leq l_{II} < 240$	0.75171	-0.57143	0.658	0.00534	12
$240 \leq l_{II} < 250$	1.97427	-2.02654	0.487	0.0	67
$250 \leq l_{II} < 260$	1.25208	-1.47763	0.424	0.31600	19
$260 \leq l_{II} < 270$	0.89448	-0.43870	1.019	0.0	05
$270 \leq l_{II} < 280$	0.81141	-0.51001	0.795	0.03505	27
$280 \leq l_{II} < 290$	0.83781	-0.44138	0.949	0.02820	50
$290 \leq l_{II} < 300$	1.10600	-0.86263	0.641	0.03402	28
$300 \leq l_{II} < 310$	1.37040	-1.02779	0.667	0.05608	28
$310 \leq l_{II} < 320$	1.77590	-1.26951	0.699	0.06972	37
$320 \leq l_{II} < 330$	1.20865	-0.70679	0.855	0.02902	35
$330 \leq l_{II} < 340$	2.28830	-1.71890	0.666	0.22887	42
$340 \leq l_{II} < 350$	3.26278	-0.94181	1.152	0.0	38
$350 \leq l_{II} < 360$	2.58100	-1.69237	0.763	0.0	53

$15 \leq b_{II} < 30$	α	β	r_0	γ	$\frac{\sigma_A}{A}$
$0 \leq l_{II} < 20$	6.23279	-10.30384	0.302	0.0	42
$20 \leq l_{II} < 40$	4.47693	-7.28366	0.307	0.0	29
$40 \leq l_{II} < 60$	1.22938	-1.19030	0.516	0.0	05
$60 \leq l_{II} < 80$	0.84291	-1.59338	0.265	0.0	04
$80 \leq l_{II} < 100$	0.23996	0.06304	0.523	0.0	32
$100 \leq l_{II} < 140$	0.40062	-1.75628	0.114	0.0	16
$140 \leq l_{II} < 180$	0.56898	-0.53331	0.523	0.0	41
$180 \leq l_{II} < 200$	-0.95721	11.69217	0.240	0.0	02
$200 \leq l_{II} < 220$	-0.19051	1.45670	0.376	0.0	01
$220 \leq l_{II} < 240$	2.31305	-7.82531	0.148	0.0	95
$240 \leq l_{II} < 260$	1.39169	-1.72984	0.402	0.0	06
$260 \leq l_{II} < 280$	1.59418	-1.28296	0.523	0.0	36
$280 \leq l_{II} < 300$	1.57082	-1.97295	0.398	0.0	10
$300 \leq l_{II} < 320$	1.95998	-3.26159	0.300	0.0	11
$320 \leq l_{II} < 340$	2.59567	-4.84133	0.268	0.0	37
$340 \leq l_{II} < 360$	5.30273	-7.43033	0.357	0.0	37

$30 \leq b_{II} < 45$	α	β	r_0	γ	$\frac{\sigma_A}{A}$
$0 \leq l_{II} < 20$	2.93960	-6.48049	0.227	0.0	77
$20 \leq l_{II} < 50$	1.65864	-9.99317	0.083	0.0	>99
$50 \leq l_{II} < 80$	1.71831	-7.25286	0.118	0.0	28
$80 \leq l_{II} < 110$	1.33617	-10.39799	0.064	0.0	>99
$110 \leq l_{II} < 160$	-0.31330	1.35622	0.329	0.0	24
$160 \leq l_{II} < 190$	1.51984	-8.69502	0.087	0.0	>99
$190 \leq l_{II} < 220$	-0.50758	4.73320	0.250	0.0	78
$220 \leq l_{II} < 250$	1.25864	-12.59627	0.050	0.0	70
$250 \leq l_{II} < 280$	1.54243	-3.76065	0.205	0.0	10
$280 \leq l_{II} < 320$	2.72258	-7.47806	0.182	0.0	05
$320 \leq l_{II} < 340$	2.81545	-5.52139	0.255	0.0	10
$340 \leq l_{II} < 360$	2.23818	0.81772	0.329	0.0	19

$45 \leq b_{II} < 60$	α	β	r_0	γ	$\frac{\sigma_A}{A}$
$0 \leq l_{II} < 60$	1.38587	-9.06536	0.076	0.0	03
$60 \leq l_{II} < 90$	2.28570	-9.88812	0.116	0.0	03
$90 \leq l_{II} < 110$	1.36385	-8.10127	0.084	0.0	04
$110 \leq l_{II} < 170$	0.05943	-1.08126	0.027	0.0	50
$170 \leq l_{II} < 200$	1.40171	-3.21783	0.218	0.0	99
$200 \leq l_{II} < 230$	0.14718	3.92670	0.252	0.0	14
$230 \leq l_{II} < 290$	0.57124	-4.30242	0.066	0.0	10
$290 \leq l_{II} < 330$	3.69891	-19.62204	0.094	0.0	05
$330 \leq l_{II} < 360$	1.19568	-0.45043	0.252	0.0	09

$60 \leq b_{II} < 90$	α	β	r_0	γ	$\frac{\sigma_A}{A}$
$0 \leq l_{II} < 30$	0.69443	-0.27600	0.153	0.0	>99
$30 \leq l_{II} < 60$	1.11811	0.71179	0.085	0.0	73
$60 \leq l_{II} < 90$	1.10427	-2.37654	0.123	0.0	>99
$90 \leq l_{II} < 120$	-0.42211	5.24037	0.184	0.0	12
$120 \leq l_{II} < 150$	0.87576	-4.38033	0.100	0.0	35
$150 \leq l_{II} < 180$	1.27477	-4.98307	0.128	0.0	72
$180 \leq l_{II} < 210$	1.19512	-6.58464	0.091	0.0	49
$210 \leq l_{II} < 240$	0.97581	-4.89869	0.100	0.0	95
$240 \leq l_{II} < 270$	0.54379	-0.84403	0.207	0.0	35
$270 \leq l_{II} < 300$	-0.85054	13.01249	0.126	0.0	39
$300 \leq l_{II} < 330$	0.74347	-1.39825	0.207	0.0	10
$330 \leq l_{II} < 360$	0.77310	-4.45005	0.087	0.0	16

This article was processed by the author using Springer-Verlag TEX A&A macro package 1992.